Iterative PET Image Reconstruction using Adaptive Adjustment of Subset Size and Random Subset Sampling

Robert Twyman, *Student Member, IEEE,* Simon Arridge, Brian F. Hutton, *Senior Member, IEEE.* Elise C. Emond, *Student Member, IEEE,* Ludovica Brusaferri, *Student Member, IEEE,* Sangtae Ahn, and Kris Thielemans, *Senior Member, IEEE*

***Abstract*—Statistical PET image reconstruction methods are often accelerated by the use of a subset of available projections at each iteration. It is known that many subset algorithms, such as ordered subset expectation maximisation, will not converge to a single solution but to a limit cycle. Reconstruction methods exist to relax the update step sizes of subset algorithms to obtain convergence, however, this introduces additional parameters that may result in extended reconstruction times. Another approach is to gradually decrease the number of subsets to reduce the effect of the limit cycle at later iterations, but the optimal iteration numbers for these reductions may be data dependent. We propose an automatic method to increase subset sizes so a reconstruction can take advantage of the acceleration provided by small subset sizes during early iterations, while at later iterations reducing the effects of the limit cycle behaviour providing estimates closer to the maximum a posteriori solution. At each iteration, two image updates are computed from a common estimate using two disjoint subsets. The divergence of the two update vectors is measured and, if too great, subset sizes are increased in future iterations. We show results for both sinogram and list mode data using various subset selection methodologies.**

I. Introduction

TRADITIONAL statistical PET reconstruction algorithms, such as maximum likelihood expectation maximisation (MLEM), converge very slowly [1]. A common acceleration methodology is to compute iterative updates using only a subset of the full measured data, thereby reducing the computational cost per update, boasting acceleration factors that are almost linearly proportional to the number of subsets during early iterations [2]. However, many subset algorithms converge to a limit cycle rather than a single solution when the number of subsets remains greater than one [1].

One solution is to use relaxation, decreasing the step-size of the update algorithm [3], [4]. While this allows the subset algorithms to converge, the rate of convergence may be slow if the relaxation parameter is poorly selected. Other methods combine the update from the current subset with those from previous subsets, leading to convergent algorithms, but at the expense of a reduced convergence rate [5]. Many authors choose to reduce the number of subsets gradually during reconstruction but often without any indication of the optimal update numbers at which to do so.

A novel algorithm that detects when the number of subsets should be decreased for future iterations was proposed by Thielemans et al. [6]. The algorithm computes two updates from the same image estimate using different subsets. Subset size is increased when a measure of the similarity between the two updates falls below a threshold. The intuition of this methodology is that, at initialisation, an ordered subset (OS) reconstruction algorithm is greatly accelerated when using smaller subsets because, during these early iterations, two different subsets' updates will be approximately equal resulting in approximately the same image estimate. However, at later iterations, significant differences between updates from two subsets may occur.

Here we propose extensions to the aforementioned algorithm by using stochastic and golden angle sampling [7] in the selection of two disjoint subsets at each iteration. Moreover, the proposed method, AutoSubsets (AS), is extended to suit list mode data using temporal subsets.

II. Methodology

The AS algorithm is a modification of standard subset iterative reconstruction algorithms and is demonstrated in this work using Block Sequential Regularised Expectation Maximisation (BSREM) [3] with the relative difference penalty [8]. At each update k of AS, two equally sized disjoint subsets B_j $(j = 1, 2)$ are selected and used to compute two image estimates x_j^{k+1} respectively. During early iterations, the size of the subsets is minimal to provide higher acceleration. The divergence of the two update directions is quantified with the cosine similarity:

$$\cos\theta = \frac{(x_1^{k+1} - x^k) \cdot (x_2^{k+1} - x^k)}{|x_1^{k+1} - x^k||x_2^{k+1} - x^k|} \tag{1}$$

and if this value falls below a threshold value $t_{\min}$, the size of the subsets is increased for future iterations. To conserve computational cost, the two subset estimates are combined into a single estimate x^{k+1}:

$$x^{k+1} = \frac{S_1 x_1^{k+1} + S_2 x_2^{k+1}}{S_1 + S_2} \tag{2}$$

Manuscript received December 13th, 2019. This research is supported by GE Healthcare, the NIHR UCLH Biomedical Research Centre and the EPSRC-funded UCL Centre for Doctoral Training in Medical Imaging (EP/L016478/1).

R. Twyman, B. Hutton, E. Emond, L. Brusaferri, and K. Thielemans are with the Institute of Nuclear Medicine, University College London, London NW1 2BU, UK (contact: `robert.twyman.18@ucl.ac.uk`).

S. Arridge is with the Centre for Medical Image Computing, University College London, Gower Street, London, WC1E 6BT, UK

S. Ahn is with GE Global Research, Niskayuna, NY, USA.

L. Brusaferri was supported by Siemens Healthineers. E. Emond was supported by GlaxoSmithKline (BIDS3000030921)

where the subset sensitivity images S_j act as weighting factors.

At each update of AS, the subsets B_j are constructed from m samples of the full data set using various sampling methodologies. The AS subsets used at each update are constrained to be disjoint to not introduce a positive bias in the cosine similarity measure.

The list mode subsets are constructed by selecting events from sequential time frames of length m from the list mode file.

Two sinogram AS sampling implementations are investigated: stochastic sampling and golden angle sampling. The stochastic sampling method constructs two subsets by randomly selecting m projection angles without replacement.

Golden angle subset selection is performed by iteratively selecting projection angles ϕ that are approximately a rotation of the golden angle $\gamma_g \approx 111.24°$ from the previously selected projection angle:

$$\phi^i \approx \phi^{i-1} + \gamma_g \mod 180° \tag{3}$$

As the scanner projection angles are fixed, ϕ^i is rounded to the nearest scanner projection angle, subject to the disjoint subset constraint.

III. Experiments

The PET scan of a large cylindrical phantom, containing four cylindrical inserts of various activities and non-uniform attenuation (Fig. 1), was simulated using GATE as a back-to-back gamma voxellised source (total activity of 101 MBq) [9]. The 120 second scan was simulated using the PET/CT GE Discovery 690 geometry and the data recorded in a list mode ROOT file. Radioactive decay was not simulated in the acquisition and reconstructions were performed without the inclusion of time-of-flight information. The open-source image reconstruction software STIR was used to read the list mode data and to implement all reconstructions [10].

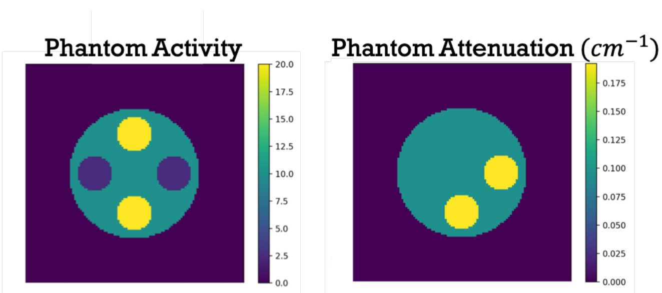

Fig. 1: The central slice of the simulated phantom activity and attenuation maps. The activity image is measured in arbitrary units.

List mode events were arranged in detection order and subsets corresponded to various time frames. For sinogram reconstruction, the data were binned into geometric projections of the scanner. A threshold $t_{\min} = 0$ was chosen and subset sizes were increased by 20% when the cosine similarity fell below this threshold. These values were chosen heuristically to correspond to a 90° divergence angle between the two updates and to allow only small increases in subset sizes.

The two sinogram based sampling methods for AS are compared to BSREM using fixed (OS) reconstructions, with various fixed subset sizes. Sinogram reconstructions initially contained 1 of the 288 projection angles per subset, and the list mode reconstruction was initialised with $1/8640^{th}$ of the full data set in each subset to use minimal computation during the early updates.

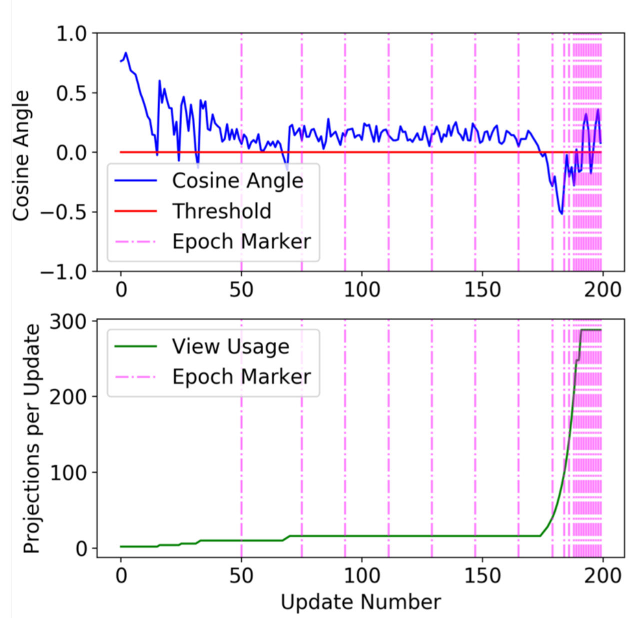

Fig. 2: Top: The cosine values of the AutoSubsets golden angle reconstruction plotted against update number. Bottom: The number of projection computations per update plotted against update number. Epoch markers are included to visualise the computational cost associated with the reconstruction.

IV. Results

The cosine similarity measures and adaptive subset sizes of the golden angle AS reconstruction are shown in Fig. 2. Algorithm performance is evaluated as objective function value with respect to computational cost, quantified as the number of gradient computation operations performed. The computational cost has been rescaled as epochs, where a single epoch is equivalent to one full pass through the data set. Objective function performance for sinogram and list mode reconstructions are plotted in Fig. 3 and Fig. 4.

V. Discussion

The proposed algorithm's cosine similarity measurements slowly decay over the initial updates (Fig. 2) and the values are measured below $t_{\min}$ after approximately 20 updates, which allows the algorithm to increase the size of the subsets. Due to the initial small subset sizes, approximately 50 updates are performed before a single epoch of the data has been processed, indicating an accelerated reconstruction. We observe a long period of approximately 100 updates with no increase in subset size, followed immediately by a sequence where nearly every update triggers an increase in subset size until the subsets contain all 288 projection angles between them. Similar behaviour was observed in all AS sinogram data reconstructions (not shown) and, while there are many potential factors that could lead to this behaviour, one possible factor is that the cosine similarity may not be the best metric

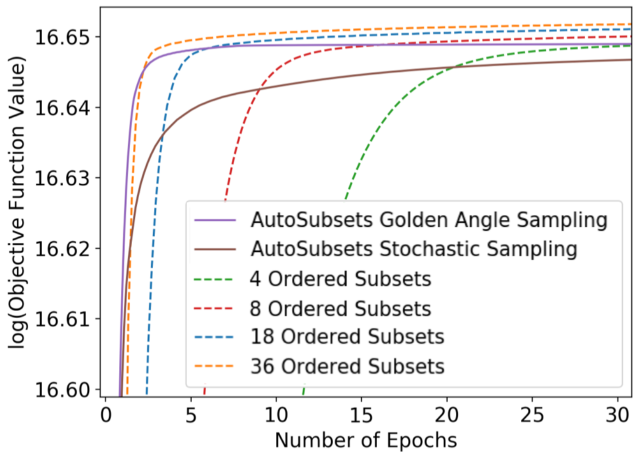

Fig. 3: Sinogram reconstructions - the logarithm of the objective function values of sequential image estimates are plotted against computational cost. AutoSubsets' performances, using the two sinogram sampling methods, are compared with four different fixed subset size BSREM reconstructions.

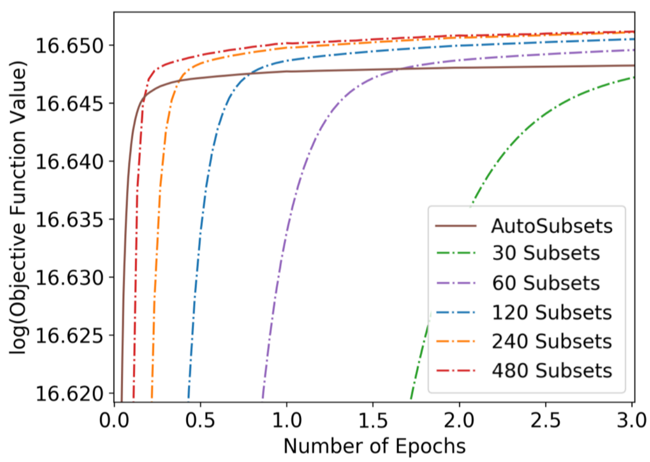

Fig. 4: List mode reconstructions - the logarithm of the objective function values of sequential image estimates are plotted against computational cost. AutoSubsets' performance is compared with five different fixed subset size BSREM reconstructions, where the list mode data were temporally binned and subsets correspond to a fixed time frames.

to determine when to increase subset sizes, especially at later updates.

The initial small subset sizes of the sinogram implementations of the AS algorithm allow for a fast increase in objective function values for the early updates (Fig. 3). The golden angle sampling algorithm achieves higher objective function values for smaller computational cost than stochastic sampling. This behaviour may be explained by the stochastic method's tendency to use larger subset sizes at earlier updates.

The AS algorithm does not outperform the OS methods for long, the '36 Ordered Subsets' objective function values do overtake the AS methods after a few epochs. Furthermore, the other OS methods also achieve greater objective function values after further computation. This indicates that the AS algorithm does not optimally determine the sizes of the subsets for each update throughout the reconstructions. It appears that the AS sinogram reconstructions are increasing subset sizes too early, consequently leading to higher computational cost and slowing the rate of convergence.

Similarly to the sinogram results, the initial small subset size of the list mode AS reconstruction allows for a rapid increase in objective function values (Fig. 4). However, the '480 Subsets' reconstruction overtakes the AS objective function values after less than half a computational epoch.

VI. Conclusion

The proposed AutoSubsets algorithm successfully increases subset sizes automatically by measuring the divergence between two update vectors at each update. Similar results were observed for both sinogram and list mode reconstructions. A notable acceleration to image reconstruction was observed during early updates, however, the algorithms objective function values were superseded by those of the fixed subset size reconstructions after the initial updates. In this study, algorithm performance is only evaluated using objective function values, which may not be the most suitable metric by which the performance of these algorithms should be measured. Future work will further explore quantitative analysis, investigate the cause of the rapid increase in subset sizes, and optimise the algorithm's hyper-parameters.

References

[1] J. Qi *et al.*, "Iterative reconstruction techniques in emission computed tomography," *Physics in Medicine and Biology*, vol. 51, R541–R578, Aug. 2006.

[2] H. M. Hudson and R. S. Larkin, "Accelerated Image Reconstruction Using Ordered Subsets of Projection Data," *IEEE Transactions on Medical Imaging*, vol. 13, no. 4, pp. 601–609, 1994.

[3] S. Ahn and J. A. Fessler, "Globally convergent image reconstruction for emission tomography using relaxed ordered subsets algorithms," *IEEE Transactions on Medical Imaging*, vol. 22, no. 5, pp. 613–626, 2003.

[4] A. R. De Pierro and M. E. B. Yamagishi, "Fast EM-like methods for maximum "a posteriori" estimates in emission tomography," *IEEE Transactions on Medical Imaging*, vol. 20, no. 4, pp. 280–288, 2001.

[5] Hsiao *et al.*, "An accelerated convergent ordered subsets algorithm for emission tomography," *Physics in Medicine and Biology*, vol. 49, pp. 2145–2156, Jul. 2004.

[6] K. Thielemans and S. Arridge, "Adaptive adjustment of the number of subsets during iterative image reconstruction," pp. 1–2, 2016.

[7] Thomas Kohler, "A projection access scheme for iterative reconstruction based on the golden section," *IEEE Nuclear Science Symposium Conference Record*, 2004.

[8] J. Nuyts *et al.*, "A Concave Prior Penalizing Relative Differences for Maximum-a-Posteriori Reconstruction in Emission Tomography," vol. 49, no. 1, pp. 56–60, 2002.

[9] S. Jan *et al.*, "GATE : a simulation toolkit for PET and SPECT," *Physics in Medicine and Biology*, vol. 49, pp. 4543–4561, 2004.

[10] K. Thielemans *et al.*, "STIR: Software for tomographic image reconstruction release 2," *Physics in Medicine and Biology*, vol. 57, no. 4, pp. 867–883, Jan. 2012.